

# Conductance Photoswitching of Metal–Organic Frameworks with Embedded Spiropyran

Shubham Garg, Heidi Schwartz, Mariana Kozłowska, Anemar Bruno Kanj, Kai Müller, Wolfgang Wenzel, Uwe Ruschewitz, and Lars Heinke\*

**Abstract:** Conductive metal organic frameworks (MOFs) as well as smart, stimuli responsive MOF materials have attracted considerable attention with respect to advanced applications in energy harvesting and storage as well as in signal processing. Here, the conductance of MOF films of type UiO 67 with embedded photoswitchable nitro substituted spiropyrans was investigated. Under UV irradiation, the spiropyran (SP) reversibly isomerizes to the open merocyanine (MC) form, a zwitterionic molecule with an extended conjugated  $\pi$  system. The light induced SP MC isomerization allows for remote control over the conductance of the SP@UiO 67 MOF film, and the conductance can be increased by one order of magnitude. This research has the potential to contribute to the development of a new generation of photoelectronic devices based on smart hybrid materials.

Conductive and semi conductive nanoporous hybrid materials attract substantial attention with respect to various applications, including chemical sensors, supercapacitors, and batteries.<sup>[1]</sup> Metal organic frameworks (MOFs), which are composed of metal nodes connected by organic linker molecules, are a subclass of crystalline, nanoporous hybrid materials.<sup>[2]</sup> Owing to their large variety and the possibility to tune their properties by designing and rationally modifying the components, MOF materials have been intensively investigated with the aim of their application as advanced semiconductors.<sup>[3]</sup> In addition, smart MOF materials with remote controllable properties can be fabricated by incorporating photoswitchable molecules,<sup>[4]</sup> such as azobenzenes, diarylethenes, or spiropyrans.<sup>[5]</sup> Azobenzene, often incorporated as a pendant group,<sup>[5c]</sup> has been used to photoswitch the absorption properties,<sup>[6]</sup> the adsorption<sup>[7]</sup> and diffusion<sup>[8]</sup>

properties of the guest molecules as well as the membrane separation performance.<sup>[9]</sup> Diarylethene moieties were used to switch the color,<sup>[10]</sup> the membrane permeation,<sup>[11]</sup> and the singlet oxygen production rates<sup>[12]</sup> of the material. So far, only a small number of publications address spiropyran in MOFs, where the photoswitch was incorporated by embedment in the pores<sup>[13]</sup> and by attachment to the framework.<sup>[14]</sup> When irradiated with UV light, the closed spiropyran (SP) form isomerizes to the open, zwitterionic merocyanine (MC) form, which goes along with an increase in the length of the molecule from 12.2 Å to 14.0 Å and an extension of the  $\pi$  electron delocalization. Upon thermal relaxation or by irradiation with visible light, MC isomerizes back to the thermodynamically stable SP form. Details of the SP MC isomerization can be found in Ref. [15]. It was demonstrated that the SP to MC isomerization results in an increase in the conductivity of single spiropyran molecules<sup>[16]</sup> and self assembled spiropyran monolayers.<sup>[17]</sup> The conductivity switching of single molecules and molecular monolayers was also shown for diarylethenes.<sup>[18]</sup> It is a major challenge to extend the conductance switching based on molecular photoisomerization to three dimensional materials. Such materials may find application as optical memories<sup>[19]</sup> and switches as well as smart sensors.

It has been demonstrated that polymers with diarylethene can be used for conductivity photoswitching, where the diarylethene may act as a hole or an electron blocking layer.<sup>[20]</sup> The effect of the diarylethene in polymer conductivity switching was amplified by using transistor setups.<sup>[21]</sup> By using spiropyran in combination with conducting polymers sensitive to the polarity of the spiropyran, a conductivity switching of a factor of 2.5 was realized.<sup>[22]</sup> Switching the electronic properties of a three dimensional material based on the delocalization of the electrons has not yet been presented. In addition, while remote control over the proton conductivity of guest molecules was recently achieved for an azobenzene containing MOF,<sup>[23]</sup> reversible photoswitching of the electronic properties of a MOF material has not yet been demonstrated.

Here, we present a photoswitchable hybrid material consisting of nitro substituted spiropyran (SP) embedded in a MOF film of UiO 67 type (Figure 1). UiO 67 was chosen as the nanoporous host structure because of its rather nonpolar pore environment without open metal sites. The nonpolar pore environment results in (closed) SP as the thermodynamically stable form,<sup>[13]</sup> which can isomerize to the (open) merocyanine (MC) form upon UV irradiation. The SP loading from solution was confirmed by X ray diffraction, UV/Vis spectroscopy, and energy dispersive X ray (EDX) spectroscopy.

[\*] S. Garg, A. B. Kanj, K. Müller, Dr. L. Heinke  
Karlsruhe Institute of Technology (KIT)  
Institute of Functional Interfaces (IFG)  
Hermann von Helmholtz Platz 1  
76344 Eggenstein Leopoldshafen (Germany)  
E mail: Lars.Heinke@KIT.edu

Dr. H. Schwartz, Prof. Dr. U. Ruschewitz  
Department of Chemistry, University of Cologne  
GreinstraÙe 6, 50939 Cologne (Germany)

Dr. M. Kozłowska, Prof. Dr. W. Wenzel  
Karlsruhe Institute of Technology (KIT)  
Institute of Nanotechnology (INT)  
Hermann von Helmholtz Platz 1  
76344 Eggenstein Leopoldshafen (Germany)

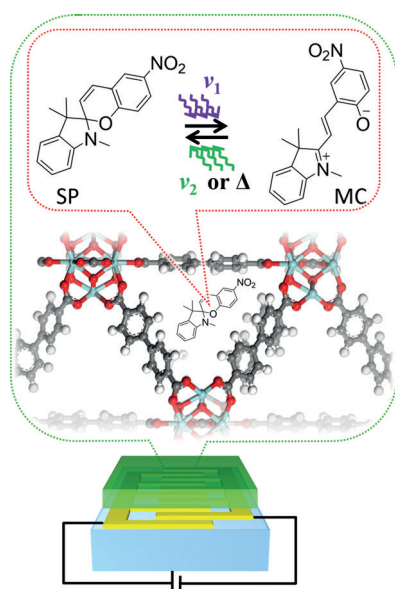


**Figure 1.** Photoswitchable MOF film with UiO 67 structure and embedded SP. C gray, H white, N blue, O red, Zr cyan. The SP MC isomerization is shown above. A SURMOF film (green) on interdigitated gold electrodes (yellow) on quartz (light blue) substrate is sketched below.

copy. For the conduction measurements, the sample was prepared on interdigitated gold electrodes on a quartz substrate. The DC conductivity measurements show an increase in the conductance by one order of magnitude upon switching from the thermodynamically stable SP form to the MC form. By thermal relaxation, MC relaxes back to SP, and the initial conductivity of the SP@UiO 67 sample is restored. This is the first demonstration of remote control over the electronic conductance of a nanoporous crystalline hybrid material.

The UiO 67 MOF films were prepared following recently published procedures.<sup>[24]</sup> The X ray diffractogram (Figure 2 a) shows that the film is crystalline with the targeted UiO 67 structure. The film is grown mainly in [111] direction, as also found in Ref. [24]. Upon loading the UiO 67 MOF film with spiropyran, the X ray diffractogram, primarily the positions and the intensity ratios of the largest peaks, remained essentially unaffected. This indicates that the sample is stable. A detailed inspection of the X ray diffractograms shows that the (220) reflection increases in intensity upon SP loading. In reference experiments with MOF powder material, a significant increase in the (220) reflection was also found upon SP loading (see Figure S9 in the Supporting Information). This change in the X ray diffraction form factor clearly indicates the SP loading in the pores. X ray diffraction peaks correlated to pure spiropyran (strongest reflection at approximately  $16.5^\circ$ ; see Figure S4a) cannot be found for the SP@UiO 67 samples, ruling out that there is a large amount of crystalline spiropyran on the external MOF surface.

Scanning electron microscopy (Figure 2c) shows the rather homogenous morphology of the film. A film thickness of approximately  $0.5\ \mu\text{m}$  was estimated from the cross sectional SEM images (Figure 2d). The EDX spectra (Figure S3) give an atomic N/Zr ratio of approximately 1:1.56. Thus, on average, there are about 15 nitrogen atoms in each

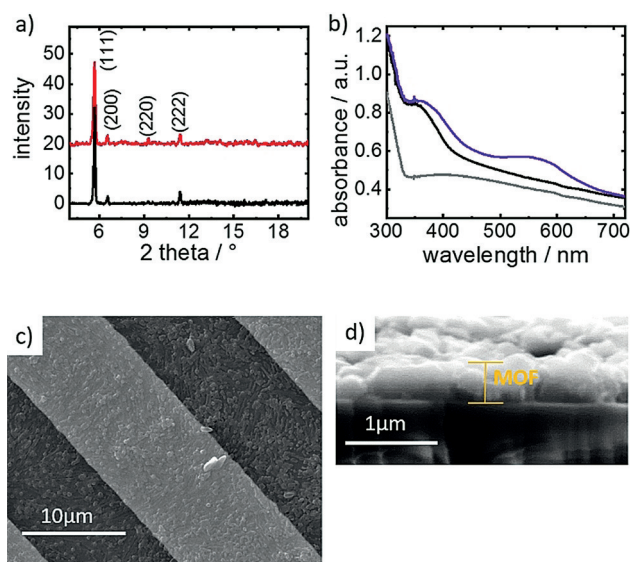


**Figure 2.** a) X ray diffractogram of the UiO 67 MOF film before (black) and after (red) loading with spiropyran. b) UV/Vis spectra of the pristine sample before loading (gray), after loading with SP (black), and after UV irradiation for 5 min (violet). Top view (c) and cross sectional image (d) of the SP@UiO 67 film on interdigitated gold electrodes recorded by SEM. The gold electrodes are visible as bright stripes in the top view. For the cross sectional measurement, the sample was broken and the fracture surface was imaged.

unit cell of  $(2.68\ \text{nm})^3$  with 24 zirconium atoms. As there are two nitrogen atoms in each spiropyran molecule and no nitrogen atoms in the MOF structure, we concluded that there are on average 7.5 spiropyran molecules embedded in each MOF unit cell. Assuming a homogenous distribution in the pores, the average (center of mass) distance between the individual molecules is  $1.37\ \text{nm}$ .

The UV/Vis absorption spectra (Figure 2b) show that an absorption band at approximately  $550\ \text{nm}$  appears upon irradiation with UV light. By comparing the UV/Vis spectrum of SP@UiO 67 with the spectrum of SP in ethanol (Figure S2a), the UV light induced band at approximately  $550\ \text{nm}$  can be clearly related to the MC form. Pure spiropyran is a crystalline solid at room temperature where the light induced SP to MC isomerization is sterically hindered. Therefore, the fact that the broad MC band at  $550\ \text{nm}$  appears upon UV irradiation, as a result of SP to MC isomerization, also indicates that the molecules are dispersed in the MOF pores.

The UiO MOF film remains colorless upon SP loading, and the SP loaded sample shows no absorption band at approximately  $550\ \text{nm}$  (resulting from MC). Thus we conclude that the pristine sample is essentially present in the SP form in the dark, and not in the MC form. The amount of MC upon UV irradiation was determined by IR vibrational spectroscopy (Figure S6): A switching yield of approximately 70% MC was achieved upon  $365\ \text{nm}$  UV light irradiation.

The conduction properties of the SP@UiO 67 sample were investigated by DC measurements (for the setup of the experiment, see Figure 1 and Ref. [23]). For this purpose, the sample was prepared on interdigitated gold electrodes,

allowing the precise measurement of the conductivity. The current as a function of time at a constant DC voltage of +1 V is shown in Figure 3a. Initially, the sample is in the thermodynamically stable SP form. Upon UV irradiation, the current increases from 0.35 nA to 3.44 nA. This means that as a result of the UV light induced SP to MC isomerization, the conductivity of the SP@UiO 67 sample increases by a factor of ten. After switching off the UV light, the MC molecules slowly isomerize back to the thermodynamically stable SP form, and an accordingly slow decrease of the current and conductivity can be observed. Simplifying the morphology of the MOF material to a homogenous defect free film of 0.5  $\mu\text{m}$  thickness, we calculated a conductivity of  $4.1 \times 10^{-9} \text{ S m}^{-1}$  for the SP form and of  $4.1 \times 10^{-8} \text{ S m}^{-1}$  for the MC form.

Three consecutive SP MC SP switching cycles are shown in Figure 3b. The current reversibly increases by approx

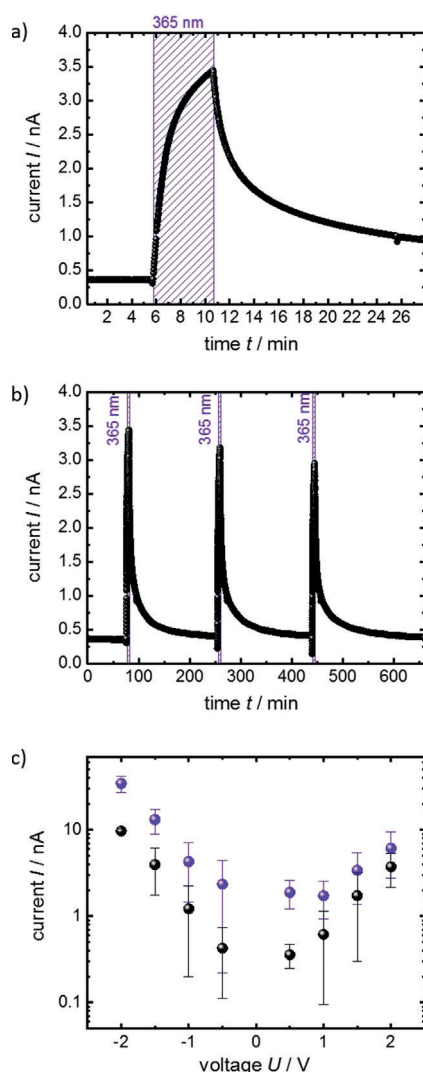


**Figure 3.** Conductance switching of SP@UiO 67 MOF. a) Current at a DC voltage of +1 V. The sample was irradiated with 365 nm UV light for 5 min. b) Current at a DC voltage of +1 V during three consecutive cycles of UV irradiation for 5 min. c) Current voltage characteristics of the sample in the SP form (black) and in the MC form (violet). The spheres with the error bars represent the average values with the standard deviations.

imately one order of magnitude upon irradiating the sample with UV light, causing SP to MC isomerization. After switching off the UV irradiation, the current slowly decreases to the initial value for SP@UiO 67. By using an exponential fit, the lifetime of the conducting (MC) form was determined to be  $24 \pm 2$  min. A small decrease in the switching effect of about 5% can be seen for the subsequent switching cycles. We assume that this decreased conductivity ratio is correlated to the fatigue of spiropyran<sup>[25]</sup> as prolonged and repetitive UV light irradiation results in photodegradation, predominantly by a bimolecular process that involves the triplet excited state of the spiropyran moiety.<sup>[26]</sup> These bimolecular processes depend on the concentration of the spiropyran molecules. This has also been found for spiropyran monolayers.<sup>[17]</sup>

The current voltage plot (Figure 3c) shows that the current significantly increase over the entire voltage range from -2 V to +2 V when the sample is switched from the SP to the MC form.

To exclude that the observed effect is caused by a potential SP film on the external MOF surface, further measurements with pure SP and MC films were carried out (Figure S4). There, no significant effect upon UV irradiation was observed. In another reference experiment, the empty UiO 67 MOF film was irradiated with UV light (Figure S5a). The conductivity of the empty sample was approximately three orders of magnitude lower than the conductivity of SP@UiO 67. Furthermore, no significant impact of the UV light on the conductivity was found. Therefore, we ascribe the observed increase in the conductance (Figure 3) to the photochromic molecules inside the MOF pores. It should be stressed that the observed effect is different to (common) photoconductivity,<sup>[27]</sup> that is, photoinduced charge carriers, where the conduction instantly starts and stops when the light is switched on or off. Such photoconduction would lead to a rectangular signal in the current time plot, which is contrary to the signal form that we obtained in our experiments (Figure 3a).

The conductance in the dark has a constant value of approximately  $4.1 \times 10^{-9} \text{ S m}^{-1}$ , and the DC current between two gold electrodes, where no protons are stored, was measured in a pure argon atmosphere so that protons as charge carriers can be excluded. The reproducibility of the conductance switching also suggests that redox reactions, for example, aryl aryl coupling of the MC isomers,<sup>[28]</sup> resulting in irreversible changes can be excluded as a reason for the change in conductance. Thus we concluded that electrons (or electron holes) are the prevailing charge carriers. This was confirmed by the admittance spectra of the sample measured over a wide frequency range (Figure S7).

To examine the details of the charge transfer, we calculated the microscopic parameters of the embedded molecules by density functional theory (DFT). In general, the mechanism of charge transfer in organic molecules, here spiropyran, is based on charge hopping rather than on ballistic transport.<sup>[29]</sup> For charge hopping transport between equal molecular levels, the conductance is proportional to  $\exp(-2\gamma r)$ , where  $r$  denotes the distance between the hopping sites and  $\gamma$  denotes the inverse wavefunction localization radius.<sup>[27b,29]</sup> Switching from SP to MC results in an increase in

the molecular extension by 1.8 Å (Figure 4a), decreasing the distance between the hopping sites  $r$  and thus increasing the conductivity. Additionally, the electron density of the frontier orbitals, (Figures 4a and S1) is more delocalized, which also leads to a decrease in the inverse wavefunction localization radius  $\gamma$ .

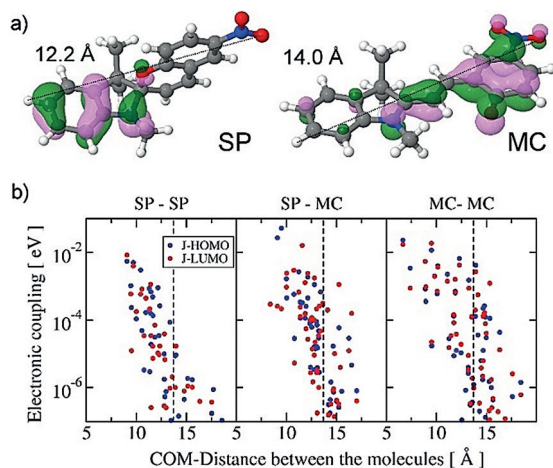


**Figure 4.** DFT calculations of microscopic parameters. a) Molecular structure of spiropyran (SP) and merocyanine (MC) with visualizations of the highest occupied molecular orbital (HOMO); the corresponding LUMOs are shown in Figure S1. b) Electronic coupling elements  $J$  between the hopping sites of spiropyran spiropyran (SP-SP), spiropyran merocyanine (SP-MC, 1:1), and merocyanine merocyanine (MC-MC) as a function of their center of mass distance (COM). Coupling elements between both HOMO and LUMO orbitals are depicted. The experimentally estimated average distance (1.37 nm) between the molecules is indicated by the dashed line.

For a better understanding of the SP/MC conductance changes, details of the charge transfer were calculated. The charge transfer in organic materials can best be described by charge hopping using Marcus theory.<sup>[30]</sup> The rate of the charge hopping between two weakly coupled sites is proportional to the square of the electronic coupling elements,  $J$ . To calculate the electronic coupling between SP, MC, and their mixture (1:1), we used the Quantum Patch approach<sup>[31]</sup> for pairs of photoswitchable molecules placed in adjacent unit cells of the MOF as described in the Supporting Information. The electronic coupling, which strongly depends on the hopping distance (Figure 4b), is in the range of 0.001–10 meV for all studied systems, enabling charge transport in the photochromic MOF film. The coupling decreases with increasing distance. At a distance between the hopping sites of 1.37 nm, which corresponds to the experimentally estimated average value, the MC-MC coupling is still relatively high, at 1–10 meV.

The electronic coupling between MC molecules is generally larger than the coupling between SP molecules, for the HOMO as well as for the LUMO orbitals (Figure 4b). While at small distances, the MC coupling for the HOMO orbitals is approximately four times larger than the SP coupling, it is roughly two orders of magnitude larger at longer molecular

distances, in particular at the experimentally estimated average value. This larger electron coupling of MC in comparison to SP results in an increased charge hopping rate. Assuming that the reorganization energies and the Gibbs free energies are not affected by the SP/MC isomerization, the larger MC coupling results in higher electronic conductance, proportional to the square of the electronic coupling element.<sup>[30]</sup> As a result, while for short molecular distances the conductance of MC is approximately 16 times higher than that of SP, the MC conductance may be up to four orders of magnitude larger than the SP conductance at large molecular distances. In the experiment, 70% of the photo switches are in the MC state, thus, most charge hops occur for MC-MC and SP-MC, explaining the measured phenomenon.

As the HOMO and LUMO of MC show similarly efficient charge transfer, we determined the ionization potential (IP) and electron affinity (EA) to evaluate whether electron or hole conduction is prevailing (see Table S1). The DFT calculations show that because of the more efficient hole injection from the gold electrode (work function of ca. 5.1 eV), the electron hole transport generally dominates, especially for MC, whose IP value is significantly (by 0.48 eV) closer to the potential of the gold electrode than the IP of SP. It should be noted that in addition to the higher coupling between the molecules, further effects might affect the electronic conductivity of the SP@UiO-67 films, such as the fact that MC is a zwitterionic molecule possessing charges with higher mobility.

Based on the results for spiropyran monolayers,<sup>[17]</sup> where conductance changes of up to a factor of 35 have been observed (with tunneling rather than hopping as the fundamental charge transfer mechanism), and based on the DFT calculations, where an even larger on/off ratio was predicted, we believe that the photoswitching effect can be further increased by optimizing the distance and the orientation of the embedded photoswitches. This could be done by optimizing the host MOF structure as well as by optimizing the structure and the loading of the photoswitches.

In conclusion, we have presented a photochromic MOF material of light responsive spiropyran embedded in UiO-67 MOF films. Upon UV irradiation, the spiropyran isomerizes to merocyanine, which goes along with changes in the microscopic properties, such as the molecular length, ionization potential, and the extension of the conjugated  $\pi$  electron system. The spiropyran to merocyanine isomerization results in a reversible increase in the electronic conductance of the spiropyran@UiO-67 MOF film by one order of magnitude. Detailed DFT calculations unveiled that the higher conductance of the merocyanine form is a result of the larger electronic coupling between the molecules and the hole injection from the gold electrode, resulting in efficient electron hole conduction.

Although the simple embedment of photochromic molecules is a straightforward way to functionalize a MOF material,<sup>[5d]</sup> the controlled immobilization of photoswitches at defined positions in the periodic framework remains a future task. This will enable precise calculations of the conduction processes in regular systems<sup>[32]</sup> and switching of the directed, anisotropic conductance.

## Acknowledgements

We thank the Volkswagenstiftung and the DFG (HE 7036/5 and SFB 1176, C6) for financial support. M.K. and W.W. acknowledge funding by M ERA.NET MODIGLIANI and SFB 1176. M.K. is very grateful to P. Friederich for fruitful discussions. This work was performed on the computational resource ForHLR II funded by the Ministry of Science, Research and the Arts of Baden Württemberg and the DFG.

## Conflict of interest

The authors declare no conflict of interest.

**Keywords:** conductivity · merocyanine · metal organic frameworks · photoswitching · spiropyrans

- [1] a) X. Lang, A. Hirata, T. Fujita, M. Chen, *Nat. Nanotechnol.* **2011**, *6*, 232; b) A. G. Slater, A. I. Cooper, *Science* **2015**, *348*, aaa8075; c) S. Demchyshyn, J. M. Roemer, H. Groß, H. Heilbrunner, C. Ulbricht, D. Apaydin, A. Böhm, U. Rütt, F. Bertram, G. Hesser, M. C. Scharber, N. S. Sariciftci, B. Nickel, S. Bauer, E. D. Głowacki, M. Kaltenbrunner, *Sci. Adv.* **2017**, *3*, e1700738.
- [2] a) H. Furukawa, K. E. Cordova, M. O'Keeffe, O. M. Yaghi, *Science* **2013**, *341*, 1230444; b) S. Kaskel, *The Chemistry of Metal Organic Frameworks: Synthesis Characterization, and Applications*, Wiley, Hoboken, **2016**.
- [3] a) M. L. Aubrey, B. M. Wiers, S. C. Andrews, T. Sakurai, S. E. Reyes Lillo, S. M. Hamed, C. J. Yu, L. E. Darago, J. A. Mason, J. O. Baeg, F. Grandjean, G. J. Long, S. Seki, J. B. Neaton, P. Yang, J. R. Long, *Nat. Mater.* **2018**, *17*, 625–632; b) I. Stassen, N. C. Burtch, A. A. Talin, P. Falcaro, M. D. Allendorf, R. Ameloot, *Chem. Soc. Rev.* **2017**, *46*, 3185–3241.
- [4] B. L. Feringa, W. R. Browne, *Molecular Switches*, Wiley, Hoboken, **2011**.
- [5] a) C. L. Jones, A. J. Tansell, T. L. Easun, *J. Mater. Chem. A* **2016**, *4*, 6714–6723; b) O. S. Bushuyev, T. Friscic, C. J. Barrett, *CrystEngComm* **2016**, *18*, 7204–7211; c) S. Castellanos, F. Kapteijn, J. Gascon, *CrystEngComm* **2016**, *18*, 4006–4012; d) H. A. Schwartz, U. Ruschewitz, L. Heinke, *Photochem. Photobiol. Sci.* **2018**, *17*, 864–873; e) A. B. Kanj, K. Müller, L. Heinke, *Macromol. Rapid Commun.* **2017**, *38*, 1700239.
- [6] S. Bernt, M. Feyand, A. Modrow, J. Wack, J. Senker, N. Stock, *Eur. J. Inorg. Chem.* **2011**, 5378–5383.
- [7] A. Modrow, D. Zargarani, R. Herges, N. Stock, *Dalton Trans.* **2012**, *41*, 8690–8696.
- [8] L. Heinke, M. Cakici, M. Dommaschk, S. Grosjean, R. Herges, S. Bräse, C. Wöll, *ACS Nano* **2014**, *8*, 1463–1467.
- [9] a) Z. Wang, A. Knebel, S. Grosjean, D. Wagner, S. Bräse, C. Wöll, J. Caro, L. Heinke, *Nat. Commun.* **2016**, *7*, 13872; b) K. Müller, A. Knebel, F. Zhao, D. Bléger, J. Caro, L. Heinke, *Chem. Eur. J.* **2017**, *23*, 5434–5438.
- [10] I. M. Walton, J. M. Cox, J. A. Coppin, C. M. Linderman, D. G. Patel, J. B. Benedict, *Chem. Commun.* **2013**, *49*, 8012–8014.
- [11] B. J. Furlong, M. J. Katz, *J. Am. Chem. Soc.* **2017**, *139*, 13280–13283.
- [12] J. Park, D. Feng, S. Yuan, H. C. Zhou, *Angew. Chem. Int. Ed.* **2015**, *54*, 430–435; *Angew. Chem.* **2015**, *127*, 440–445.
- [13] H. A. Schwartz, S. Olthof, D. Schaniel, K. Meerholz, U. Ruschewitz, *Inorg. Chem.* **2017**, *56*, 13100–13110.
- [14] a) K. Healey, W. B. Liang, P. D. Southon, T. L. Church, D. M. D'Alessandro, *J. Mater. Chem. A* **2016**, *4*, 10816–10819; b) D. E. Williams, C. R. Martin, E. A. Dolgoplova, A. Swifton, D. C. Godfrey, O. A. Ejegbavwo, P. J. Pellechia, M. D. Smith, N. B. Shustova, *J. Am. Chem. Soc.* **2018**, *140*, 7611–7622.
- [15] R. Klajn, *Chem. Soc. Rev.* **2014**, *43*, 148–184.
- [16] N. Darwish, A. C. Aragones, T. Darwish, S. Ciampi, I. Diez Perez, *Nano Lett.* **2014**, *14*, 7064–7070.
- [17] S. Kumar, J. T. van Herpt, R. Y. N. Gengler, B. L. Feringa, P. Rudolf, R. C. Chiechi, *J. Am. Chem. Soc.* **2016**, *138*, 12519–12526.
- [18] a) Y. Kim, T. J. Hellmuth, D. Sysoiev, F. Pauly, T. Pietsch, J. Wolf, A. Erbe, T. Huhn, U. Groth, U. E. Steiner, E. Scheer, *Nano Lett.* **2012**, *12*, 3736–3742; b) N. Katsonis, T. Kudernac, M. Walko, S. J. van der Molen, B. J. van Wees, B. L. Feringa, *Adv. Mater.* **2006**, *18*, 1397–1400.
- [19] D. A. Parthenopoulos, P. M. Rentzepis, *Science* **1989**, *245*, 843–845.
- [20] R. C. Shallcross, P. Zacharias, A. Koehnen, P. O. Koerner, E. Maibach, K. Meerholz, *Adv. Mater.* **2013**, *25*, 469–476.
- [21] a) M. E. Gemayel, K. Borjesson, M. Herder, D. T. Duong, J. A. Hutchison, C. Ruzie, G. Schweicher, A. Salleo, Y. Geerts, S. Hecht, E. Orgiu, P. Samori, *Nat. Commun.* **2015**, *6*, 6330; b) E. Orgiu, N. Crivillers, M. Herder, L. Grubert, M. Patzel, J. Frisch, E. Pavlica, D. T. Duong, G. Bratina, A. Salleo, N. Koch, S. Hecht, P. Samori, *Nat. Chem.* **2012**, *4*, 675–679.
- [22] G. Jiang, Y. Song, X. Guo, D. Zhang, D. Zhu, *Adv. Mater.* **2008**, *20*, 2888–2898.
- [23] K. Müller, J. Helfferich, F. L. Zhao, R. Verma, A. B. Kanj, V. Meded, D. Bléger, W. Wenzel, L. Heinke, *Adv. Mater.* **2018**, *30*, 1706551.
- [24] E. Virmani, J. M. Rotter, A. Maehringer, T. von Zons, A. Godt, T. Bein, S. Wuttke, D. D. Medina, *J. Am. Chem. Soc.* **2018**, *140*, 4812–4819.
- [25] A. Tork, F. Boudreault, M. Roberge, A. M. Ritcey, R. A. Lessard, T. V. Galstian, *Appl. Opt.* **2001**, *40*, 1180–1186.
- [26] M. Sakuragi, K. Aoki, T. Tamaki, K. Ichimura, *Bull. Chem. Soc. Jpn.* **1990**, *63*, 74–79.
- [27] a) A. D. Schwab, D. E. Smith, B. Bond Watts, D. E. Johnston, J. Hone, A. T. Johnson, J. C. de Paula, W. F. Smith, *Nano Lett.* **2004**, *4*, 1261–1265; b) D. Hertel, H. Baessler, *ChemPhysChem* **2008**, *9*, 666–688.
- [28] O. Ivashenko, J. T. van Herpt, P. Rudolf, B. L. Feringa, W. R. Browne, *Chem. Commun.* **2013**, *49*, 6737–6739.
- [29] N. Tessler, Y. Preezant, N. Rappaport, Y. Roichman, *Adv. Mater.* **2009**, *21*, 2741–2761.
- [30] R. A. Marcus, *Rev. Mod. Phys.* **1993**, *65*, 599–610.
- [31] a) P. Friederich, V. Meded, A. Poschlad, T. Neumann, V. Rodin, V. Stehr, F. Symalla, D. Danilov, G. Luedemann, R. F. Fink, I. Kondov, F. von Wrochem, W. Wenzel, *Adv. Funct. Mater.* **2016**, *26*, 5757–5763; b) P. Friederich, F. Symalla, V. Meded, T. Neumann, W. Wenzel, *J. Chem. Theory Comput.* **2014**, *10*, 3720–3725.
- [32] T. Neumann, J. Liu, T. Waechter, P. Friederich, F. Symalla, A. Welle, V. Mugnaini, V. Meded, M. Zharnikov, C. Wöll, W. Wenzel, *ACS Nano* **2016**, *10*, 7085–7093.